DELPHI Collaboration

DELPHI 98-38 CONF 128
24 April, 1998

Update of the search for charginos mass-degenerate with the lightest neutralino in radiative events

S. Paiano, A. Perrotta, T. Rovelli
INFN and Università - Bologna

Abstract

The data collected by DELPHI in 1997 at the centre-of-mass energies of 183, 130 and 136 GeV have been used to search for charginos mass-degenerate with the LSP. A photon radiated from the initial state improves the trigger efficiency of the signal and allows its separation from the background. No evidence of excess above the expectation from standard processes has been found at any of the centre-of-mass energies inspected. When complemented with the already reported non observation of that signal in the previous LEP2 runs, this result tightens the lower limits on the mass of the chargino, when the mass difference between it and the lightest neutralino is between 0.3 and 3 GeV/c^2, in all the scenarios in which such a degeneracy can be present.

1 Introduction

This note updates the results of the search for degenerate charginos in radiative events, reported in [1], with the data collected by DELPHI in 1997 at the three centre-of-mass energies of 130, 136 and 183 GeV. The mass splitting between the chargino and the lightest neutralino (supposed to be the LSP) of interest for this analysis lies between 0.3 and 3.0 GeV/c^2: in this region the usual searches for charginos [2] loose efficiency. The addition of the new statistics increases the significance of this low efficiency search, allowing the search for mass-degenerate charginos also in scenarios not touched in the previous analysis.

The Higgsino and gaugino sector of the minimal SUSY can be described in term of four parameters: the ratio $\tan\beta$ of the two Higgs vacuum expectation values, the Higgs mixing parameter μ, the SU_2 gaugino mass M_2 and the U_1 gaugino mass M_1. The lightest chargino is mass-degenerate with the LSP in two cases [3]:

- Low μ, large $M_{1,2}$ scenario: $\tilde{\chi}^0_1$ and $\tilde{\chi}^+_1$ are both higgsino-like and nearly degenerate, with masses $\sim \mu$;
- High μ, low M_2: the $\tilde{\chi}^0_1$ and the $\tilde{\chi}^+_1$ are both gaugino-like and degenerate with masses $\sim M_2$. In this scenario, in order to have $\Delta(M)$ of the order of 1 GeV/c^2 or lower, M_1 must be bigger than, or approximately equal to, M_2

The second scenario implies that there is no gaugino mass unification at the GUT scale, since it would give a relation between the masses of the gauginos like:

$$M_1 = \frac{5}{3}\tan^2\theta_W \cdot M_2 \simeq 0.5 \cdot M_2 \quad . \tag{1}$$

The dependence of the cross-sections and the branching ratios from the SUSY parameters in the two scenarios has been estensively studied in [1]. In the higgsino case the cross section, at a given centre-of-mass energy, depends only on the mass of the chargino; in the gaugino case it depends also on the other SUSY parameters, the most relevant being the mass of the sneutrino (the exchange of sfermions in the t-channel interferes destructively with the s-channel exchange, lowering the gaugino cross section at small values of $M(\tilde{\nu})$). In the previous work one could set only a limit in the gaugino scenario, in correspondence of an heavy sneutrino ($M(\tilde{\nu}) > 500$ GeV/c^2). With the present statistics, lower limits on the mass of the chargino can be set also in the higgsino scenario and in the gaugino scenario with low $M(\tilde{\nu})$. In figure 1 are shown the cross sections at $\sqrt{s} = 183$ GeV for the three cases outlined above.

Figure 2 shows the chargino branching ratios and lifetimes, in the approximation of heavy sneutrinos and as a function of $\Delta(M)$. They are different with respect to those already used in [1], that where taken from [3]. Since then, the authors of [3] discovered a serious bug in their calculation of the chargino decay widths [4]. In fact, the decay modes into an odd number of pions were not considered, at first, leading to a huge underestimation of the total decay width for $\Delta(M)$ approximately comprised between 150 MeV/c^2 and 1 GeV/c^2.

Since $\tilde{\chi}^+_1 \to \tilde{\chi}^0_1\pi^+$ is a two body decay, another consequence of the new calculation of the decay modes is that its visible products are more energetic, at a given $\Delta(M)$, than the corresponding visible decay products of a three body decay. This forced to reconsider

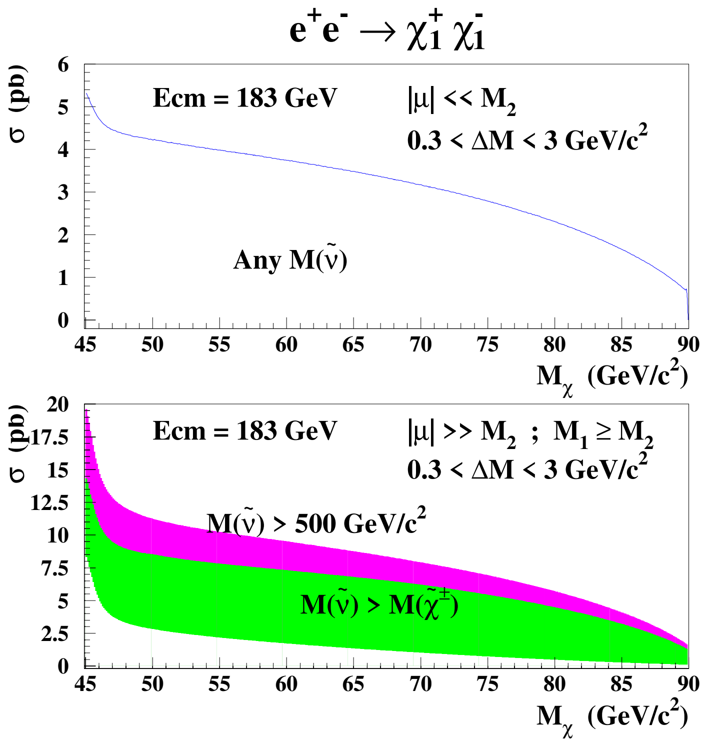

Figure 1: *$e^+e^- \to \tilde{\chi}_1^+\tilde{\chi}_1^-$ cross sections at the centre-of-mass energy of 183 Gev as a function of the mass of the chargino. The upper plot refers to the $|\mu| \ll M_2$ higgsino-like scenario; the lower plot to the $M_2 \ll |\mu|$ gaugino-like scenario. The widths of the bands allow also for a variation of M_1, M_2 and μ so that $0.5 < \Delta(M) < 3$ GeV/c^2; $1 < \tan\beta < 50$; $M_2 \leq 2M_1 \leq 10M_2$; $M(\tilde{\nu}) > M(\tilde{\chi}_1^\pm)$ (while the upper part of the gaugino band displays separately the points corresponding to $M(\tilde{\nu}) > 500$ GeV/c^2).*

all the simulations previously done at the centre-of-mass energies already reported in [1], in order to get the correct signal efficiencies. In the mean while, it has been possible to study intervals of $\Delta(M)$ down to 300 MeV/c^2 (instead of 500 MeV/c^2 as before) in the higgsino scenario and in the gaugino scenario with heavy sneutrinos, thanks to the increased energy of the visible decay products.

2 Data samples and event generators

The luminosities collected by DELPHI in 1997 at all energies above the Z^0 peak and used in the present analysis amount to 49.3 pb^{-1} at centre-of-mass energies between 182 and 184 GeV; 3.0 pb^{-1} at 130 GeV; 2.9 pb^{-1} at 136 GeV. These numbers already account for the rejection of all the runs in which the subdetectors relevant for the analysis do not work with a sufficient efficiency.

To evaluate the signal efficiency and the background contamination, events are generated using several programs, all relying on JETSET 7.4 [5] for quark fragmentation. All generated events pass through a complete simulation of the DELPHI detector [6], and are then processed in the same way as the real data.

The program SUSYGEN 2 [7], which includes ISR and FSR, is used to simulate the

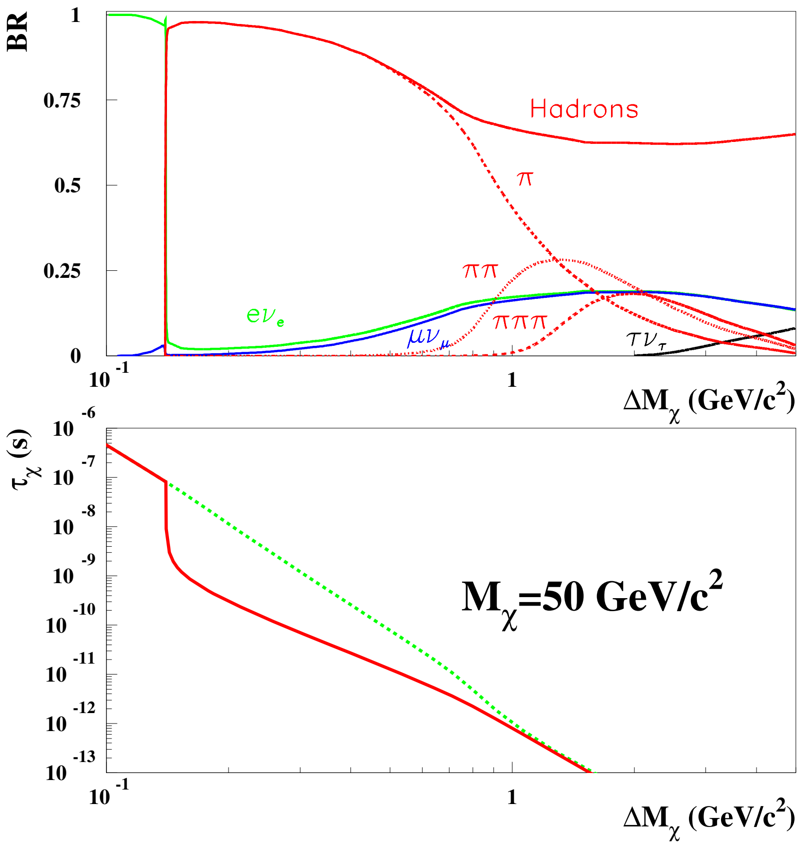

Figure 2: *Branching ratio and lifetime of a 50 GeV/c^2 chargino as a function of $\Delta(M)$, in the approximation of heavy sneutrinos. In the first plot, dashed are the contributions to the total hadronic branching ratio (full line) of the decays into a $\tilde{\chi}_1^0$ and one, two and three π. In the lifetime plot is shown the comparison with the previous (wrong) calculation in [3], who neglected the decays into a neutralino and an odd number of pions below approximately $\Delta(M) = 1.4$ GeV/c^2.*

signal: $e+e- \to \tilde{\chi}_1^+\tilde{\chi}_1^-$ events were generated at $\sqrt{s} = 183.2$ GeV with chargino masses of 45, 50, 60 and 70 GeV/c^2 and mass differences of the order of 0.3 (0.5 in case of gauginos with light sneutrinos), 1 and 3 GeV/c^2.

For the SM background, several samples of the different final states were generated with statistics which is more than twice (in the worst cases) the one expected, a part the VDM sample in which the number of events simulated so far is only slightly higher than the number of events expected with the luminosity collected in 1997. Radiative Z^0 decays and four-fermion processes are generated with PYTHIA [5]. For the $\gamma\gamma$ collisions, the BDK generator [8] is used for the leptonic final states, where in the $(e^+e^-)\mu^+\mu^-$ and in the $(e^+e^-)\tau^+\tau^-$ final states is included the simulation of the transverse energy of the ISR photon, while in the $(e^+e^-)e^+e^-$ it is not. In the $\gamma\gamma$ collisions leading to hadronic final states, the QCD and VDM parts are simulated using the TWOGAM [9] generator (which has no transverse energy associated to the ISR photon), while BDK with visible ISR is used for the QPM part.

The signal efficiencies for the centre-of-mass energies of 130 and 136 GeV are derived by multiplying the ones already computed for the 1995 data times a conservative dumping factor, which takes into account the reduction in trigger and selection efficiency observed when moving between the two samples.

3 Event selection

The criteria used to select events are defined on the basis of the simulated signal and background. The analysis of the previous years data, as reported in [1], has been combined with the new one.

With respect to the old event selection, some new feature has been added in the analysis of data collected in 1997, profiting of a new tool [10] developed to search for hits in the VD/VFT associated to the photon candidate. This tool allows a much better e/γ separation, especially in the critical region between 10^0 and 25^0 where there is no TPC coverage and the reconstruction efficiency for charged particles drops.

Charged particles with momentum above 100 MeV/c, are accepted provided $\Delta p/p <$ 100%, the impact parameter is below 4 cm in $r\phi$ and below 10 cm in z and the track length is at least 30 cm. To reduce the incidence of beam-gas or other spurious events, a primary vertex compatible with the beam spot must be reconstructed by using at least two of the charged particles.

Neutrals must have an energy of at least 500 MeV. Both calorimetric deposits and clear photon conversions, as reconstructed by the ELEPHANT package [11], are considered. To reduce the amount of spurious showers in the calorimeters faking a neutral particle in the event, the following criteria are used. In the HPC at least three consecutive layers must be hit; the shower must start before the 6^{th} HPC layer; not more than 90% of the total energy of the shower can be deposited in a single layer; the θ angle recostructed in the calorimeter must point to the main event vertex within 15^o. For the neutrals in the FEMC is defined a frame of 3×3 glasses, centered on the baricenter of the shower. The neutral is discarded if it has more than 8 GeV and more than 94% of its energy is deposited in the central glass, or if it has not more than three glasses hit and they are all lined up in a row or in a column. In the STIC an energy of more than 2 GeV must be associated to the shower and at least two towers must be hit.

All neutral showers inside a cone with half opening angle of 5^o are recombined together. If, after the recombination, the resulting neutral gets a fraction of hadronic energy above 10% of its total energy it will not be considered as an ISR photon candidate.

All particles not having associated hits in any of the tracking devices of DELPHI have been taken as neutrals. Given the lower reconstruction and association efficiency of tracks in the two endcaps of DELPHI with respect to the barrel, tag electrons from $\gamma\gamma$ events can be seen as calorimetric deposits without the corresponding track elements: if such electrons are isolated, they can fake ISR photons, and special care must be paid to cope with those events. In the following, 'photon candidate' will mean a particle without track elements attached to it, not necessarily a 'real photon'.

The complete list of selection criteria applied on the 1997 data is the following.

- The transverse energy of the photon, E_T^γ, must exceed $0.0329 \cdot \sqrt{s}$, according to the formula given in eq. (1) of [1].

- The mass recoiling against the photon (M_{opp}) must be above 96 GeV/c^2 (this is nothing else than an upper bound on the energy of the photon).
- The photon must be isolated by at least 30^o with respect to any other charged or neutral particle in the event.
- There must be at least 2 and at most 6 charged particles in the event
- The visible energy of the event, excluding the photon, must be below 5% of E_{cms}. In the search for the lowest $\Delta(M)$'s considered here ($0.3 < \Delta(M) < 1$ GeV/c^2 or $0.5 < \Delta(M) < 1$ GeV/c^2) this cut is reduced to 2%.
- The fraction of visible energy inside a double cone of 30^o (E_{30}/E_{vis}) or a single hemisphere cone of 60^o (E_{Frw}/E_{vis}), both centered on the beam axis, must be below, respectively, 25% and 99%. If the photon is inside the cone, its energy is subtracted both from the numerator and from the denominator defining those fractions.
- If the ISR photon candidate is in the STIC region, it must be antitagged by the Veto Counters scintillators placed in front of the STIC, according to the algorithm described in [12].
- If the ISR photon candidate lies between 10^o and 25^o, there must be no hits in the VD or in the Forward Tracker along its trajectory from the beam spot to the FEMC shower [10].

With respect to the selection in [1]: the upper limit on the charged multiplicity has been added (this is transparent for the signal but useful for the rejection of hadronic $\gamma\gamma$'s); the VD/VFT tag has been added; for the charge tag in the STIC the tool which will become official has been substituted to the previous 'private' one; the fraction of energy allowed in the forward double cone has been lowerd to allow a better $\gamma\gamma$ rejection, while for the single emisphere the only request remained is that not all particles can be in the same DELPHI side in a 60^o cone centered on the beam; the cut on aplanarity (that resulted to be effective at the lower LEP2 energies but not at all energies above 161 GeV, see also [1]) has been removed.

The STIC Veto and the VD/VFT tag are not properly included in the standard DELPHI detector simulation. The performances of the two algorithms on the 1997 data can be found in [12] and [10], respectively; they have been verified using a sample of Comptons which reproduces the features of the showers selected for this analysis. In particular, with photons emitted in the 10^o-25^o region, the efficiency of the VD/VFT tag for the real photons has been measured. This is shown in figure 3, where the photon (in)efficiency of the algorithm in 1997 has been parametrized as:

$$1 - \varepsilon_{\gamma}^{VD/VFT} = \max(\eta_{min},\ 0.628 - 0.0255 \cdot \min(\theta_{\gamma}, 180 - \theta_{\gamma})) \tag{2}$$

for $10^o < \min(\theta_{\gamma}, 180 - \theta_{\gamma}) < 25^o$, θ_{γ} in degrees. η_{min} is the level of fake associations, measured by looking at the response to isolated random vectors inserted in the data themselves; it ranges between 1.5 and 2.5% in the region of polar angles of interest.

Figure 4 shows the comparison of the distributions of the variables relevant for the analysis between the data and the sum of all SM expectations for the 183 GeV preselected sample, compared with the corresponding distributions in some of the signal samples. The

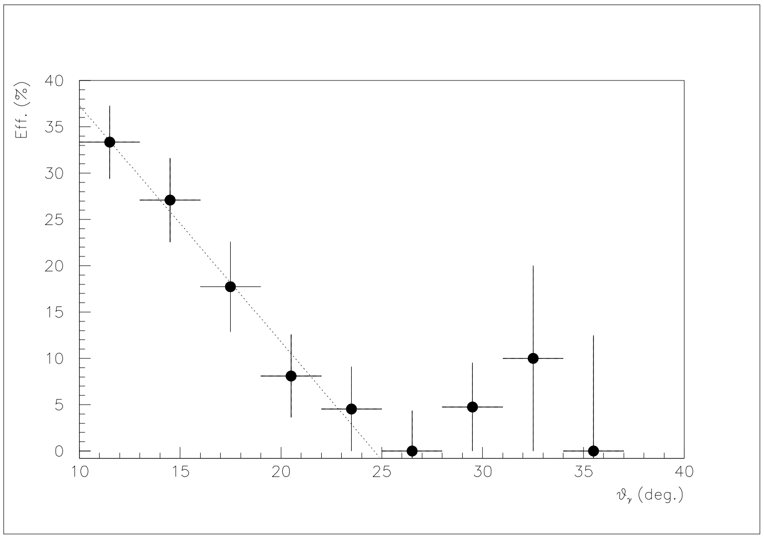

Figure 3: *Inefficiency of the VD/VFT photon tag in the FEMC region, measured with real photons coming from Compton events selected during the high energy runs in 1997.*

preselection requires a photon with $E_T^\gamma > 4.6$ GeV and $M_{opp} > 90$ GeV/c^2, isolated by more than 15^o from any other charged or neutral particle in the event, accompanied by at least two and at most 10 charged particles, the total visible energy (excluding the candidate photon) below 8% of the centre-of-mass energy, the fraction of energy within 30^o to the beam pipe below 60% and not all particles in the same 60^o emisphere centered on the beam axis. The agreement is reasonable, although, as already observed in the data at 161 and 172 GeV, there is an excess in the data when the visible energy (excluding the candidate photon) is below 1% of the centre-of-mass energy. As in the past, it is reasonable to guess that the standard background is underestimated there, mainly due to the lack of high p_T ISR photons in some of the generators but also to some cut already present at the generator level in order to keep the number of simulated events within a manageable size.

No detailed study of the background has been done for the points collected at the centre-of-mass energies of 130 and 136 GeV: most of the simulation is not readily available and, a posteriori, since no candidates has been found at those energies there is no need to have a precise evaluation of the background content there to set the limits.

4 Results

Table 1 shows the effect of the cuts on data and standard MC at the centre-of-mass energy of 183 GeV, and on data only for the runs at 130 and 136 GeV. The last column of the table refers to the tighter cut on the fractional energy carried by all particles but the candidate ISR photon: this will be used to derive more stringent limits on the mass of the chargino in the most degenerate case considered here, once no excess is evident after the previous cuts. The effect of the charge tags in the STIC scintillators and VD/VFT in the MC samples are taken into account by weighting the events with the efficiency coefficients derived from the data themselves. Also the trigger efficiency is considered through weighting coefficients applied to the MC (see below).

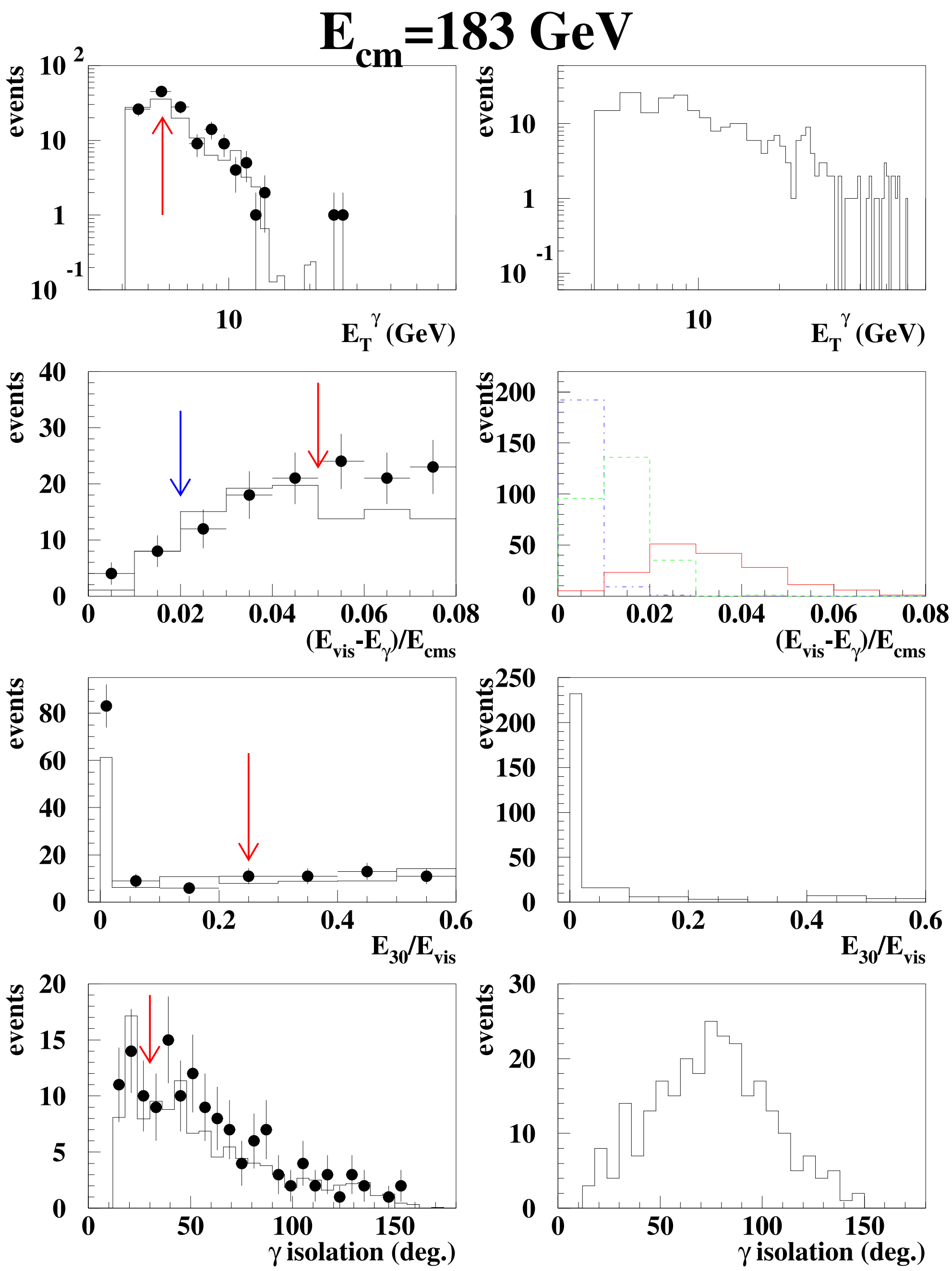

Figure 4: *Some of the variables used in the selection at 183 GeV. In the left plots the data (dots) are compared with the SM expectations. On the right, as an example, the corresponding distributions (with arbitrary normalization) are shown for the signal of mass 50 GeV/c^2 and $\Delta(M)$ = 1 GeV/c^2. In the plot of the visible energy all the three degeneracies are shown for M_χ = 50 GeV/c^2: dotted-dashed, $\Delta(M)$ = 0.3 GeV/c^2; dashed, $\Delta(M)$ = 1 GeV/c^2; full line, $\Delta(M)$ = 3 GeV/c^2.*

	E_γ^T,M_{opp}	low angles	γ isol.	$\frac{E_{vis}-E_\gamma}{E_{cms}} < 5\%$	$\frac{E_{vis}-E_\gamma}{E_{cms}} < 2\%$
E_{cms} = 130/136 GeV					
Data	2	2	0	0	0
E_{cms} = 183 GeV					
$Z^0\gamma \to q\bar{q}\gamma$	0.17	0.17	0.15	–	–
$Z^0\gamma \to \tau^+\tau^-\gamma$	0.20	0.20	0.20	$0.07 \pm .06$	$0.01 \pm .01$
$l\nu l\nu$	0.13	0.10	0.10	$0.06 \pm .04$	$0.03 \pm .03$
$e\nu q\bar{q}$	0.04	–	–	–	–
$\nu\nu q\bar{q}$	0.01	0.01	0.01	–	–
$\gamma\gamma \to e^+e^-$	0.33	0.31	–	–	–
$\gamma\gamma \to \mu^+\mu^-$	0.07	0.07	0.07	$0.01 \pm .01$	–
$\gamma\gamma \to \tau^+\tau^-$	1.88	1.56	0.65	$0.40 \pm .10$	$0.05 \pm .03$
$\gamma\gamma \to$ hadr. (VDM)	4.97	1.50	0.76	$0.76 \pm .62$	$0.15 \pm .09$
$\gamma\gamma \to$ hadr. (QPM)	2.43	2.23	1.42	$1.08 \pm .46$	$0.18 \pm .18$
$\gamma\gamma \to$ hadr. (QCD)	1.76	1.17	0.53	$0.53 \pm .38$	–
Σ backgrounds	12.2	7.3	3.9	$2.92 \pm .87$	$0.43 \pm .21$
Data	17	9	6	4	2

Table 1: *Effect of the selection cuts on the data and on the expected SM background in the sets of data collected during 1997. For 130 and 136 GeV no detailed study of the background has been done, see text.*

After the cuts, four candidates remain in the runs at centre-of-mass energies around 183 GeV, where 2.92 ± 0.87 are expected from standard processes; no candidate remains in the 1997 runs at 130/136 GeV. After the tightening of the cut on the visible energy, just two candidates remain in the runs at 183 GeV, where 0.43 ± 0.21 are expected; moreover, also the candidate at $\sqrt{s} = 172$ GeV reported in [1] cancels out after that cut (the SM expectations for the data at 161 and 172 GeV after the last cut are 0.20 and 0.08 events respectively). Table 2 lists some of the quantities relevant in the selection for the four candidates of 1997 and, for completeness, also for the candidate of 1996 described in [1].

Run	Event	E_γ	θ_γ	E^T_γ	$\frac{E_{vis}-E_\gamma}{E_{cms}}$
$E_{cms} = 172$ GeV					
71472	389	7.9 GeV	56.8^o	6.6 GeV	3.5%
$E_{cms} = 183$ GeV					
75812	19	53.4 GeV	10.6^o	9.8 GeV	0.5%
77755	372	8.4 GeV	52.2^o	6.6 GeV	1.8%
77777	20902	7.0 GeV	124.9^o	5.8 GeV	3.3%
80332	24575	5.8 GeV	85.5^o	5.7 GeV	4.1%

Table 2: *List of all the candidates remaining after the selection cuts at all centre-of-mass energies of LEP2.*

As already observed in the preselected sample (fig. 4), there is a small excess of data above the SM expectations, limited to the lowest visible energies at 183 GeV. The most probable explanation of such an excess, already seen also in the data of the previous year (although it cancelled out completely there after the final cuts) is the one guessed in the previous paragraph.

The selection efficiency for degenerate charged higgsinos and gauginos at $\sqrt{s}$ = 183 GeV, in correspondence of the cut $(E_{vis} - E_\gamma)/E_{cms} < 0.05$, estimated by using the samples of MC generated events, is shown in figure 5 as a function of the mass of the chargino and of $\Delta(M)$. It must be stressed that the very low signal efficiency comes from the necessary requirement of having a hard ISR photon radiated at visible angles: when the mass of the chargino increases, the ISR photon becomes softer, thus lowering the overall event selection efficiency.

A more precise study with respect to [1] leads to the conclusion that the efficiency for gauginos is higher than that for higgsinos: in spite of the fact that the events are similar in the two scenarios, the gaugino cross section resonates stronger around the Z pole, leading to a more frequent ISR radiation. This fact was not taken into account into the previous note; however, since all the efficiencies were computed there by using samples of simulated higgsinos, the results were conservative in the gaugino scenario. In the present study, a multiplicative factor, which depends also on the mass of the chargino, is applied to the efficiencies computed with the higgsinos when used for the gauginos, in order to take into account the increased rate of ISR radiation. A similar factor, which depends further on the centre-of-mass energy, is applied to rescale the gaugino efficiencies computed in the past analysis.

Moreover, the gaugino efficiency is significantly smaller than the one shown in the plot when the mass of the sneutrino is close to the mass of the chargino: light sneutrinos would enhance the fraction of leptonic decays, which have additional missing energy and then a lower efficiency for the same $\Delta(M)$.

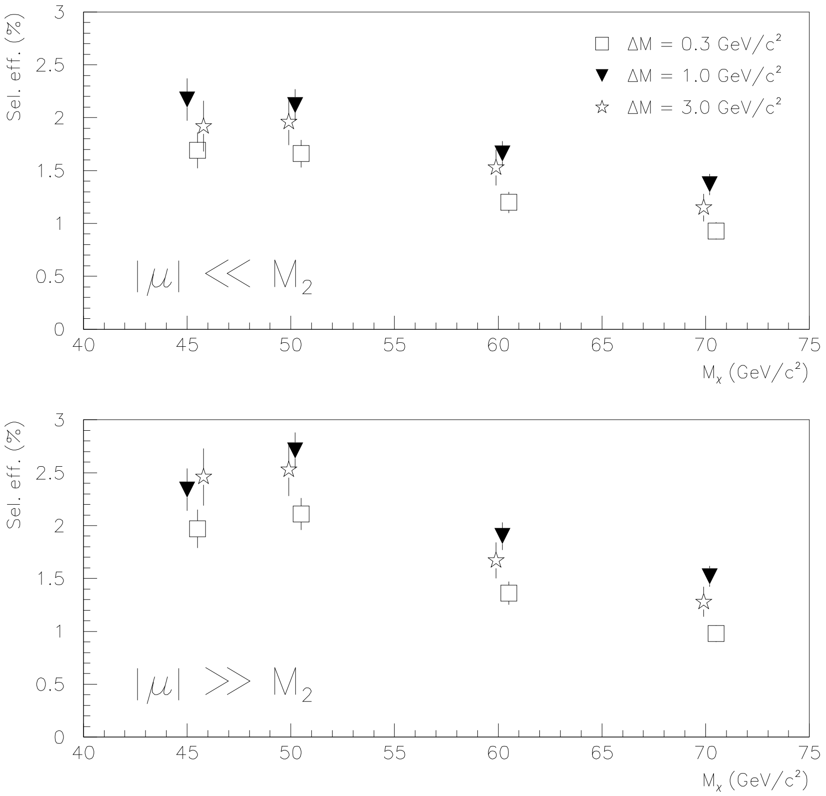

Figure 5: *Selection efficiencies for charged higgsinos and gauginos at 183 GeV as a function of their mass and mass difference with the lightest neutralino. This gaugino efficiency is valid only in the approximation of heavy sneutrinos; for light sneutrinos a different value is used.*

The trigger efficiency in DELPHI is practically 100% for most of the accessible final states. However, in the present search one looks for few particles of very low momentum, accompanied by an energetic photon. Below transverse momenta of the order of 1-2 GeV/c the single track trigger efficiency starts to decrease [13]. That's why for the present analysis a dedicated and detailed study of the trigger performances at low visible and trasverse energy has been carried out. The trigger efficiencies for events having a visible and transverse energy similar to the one of the system accompanying the ISR photon in the signal samples have been computed using all the high energy data collected in 1997. This study must be repeated for every new year of data taking, since the definition of the decision functions and the downscaling factors applied in case of noise during the data acquisition change quite often. All events triggered independently by any of the calorimeters represent the sample from which to compute the trigger efficiency for the tracking components. Figure 6 shows the track trigger efficiency in DELPHI for events with just two charged particles at polar angles above 40^o, as a function of the mean charged transverse energy of the event. It has been parametrized as

$$w_{low\,p_T} = 0.965 - 0.847 \cdot e^{-\left(\frac{E^T_{mean}}{0.808}\right)^2} \tag{3}$$

to get the weighting factors for the MC's.

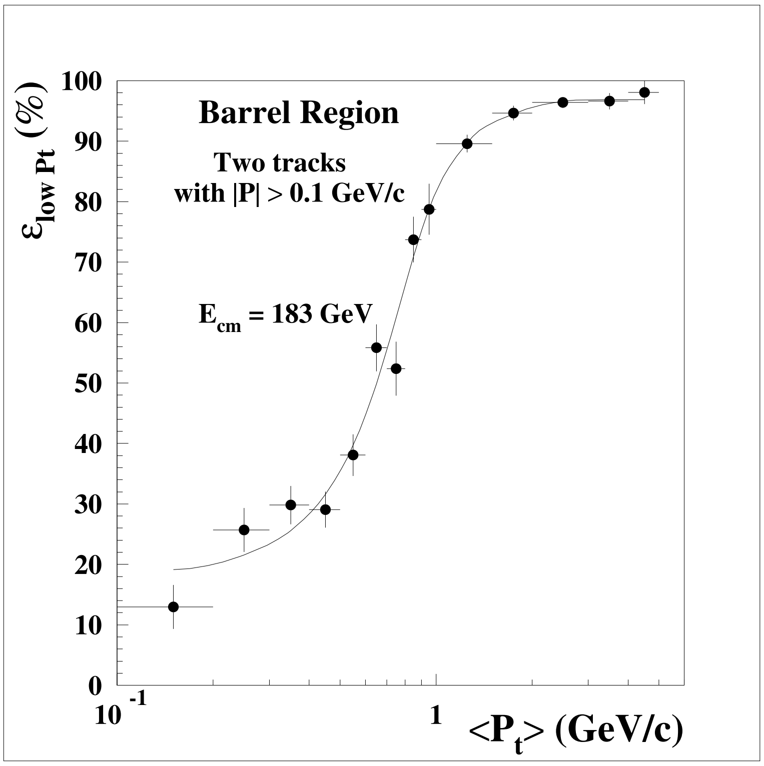

Figure 6: *Trigger efficiency in the tracking devices of DELPHI for events with two particles at low total visible energy, as a function of the mean charged transverse energy of the event. The result of the fit is superimposed.*

The overall trigger efficiency for the signal is then estimated as the logical OR of the known single photon trigger efficiency [14, 12] and the low momentum trigger efficiency. Such an estimate is certainly conservative, because no calorimetric components have been taken into account when computing the low p_T trigger efficiency and also because the coincidence of the hard photon and some of the remaining signals can, sometimes, generate a further independent trigger signal. In the range of signals considered here, the estimates of the overall trigger efficiency vary between 85% and 98%.

5 Exclusion limits

Since there is no evidence for a signal at any of the centre-of-mass energies studied here and in [1], one can derive limits on the production of pairs of charginos mass-degenerate with the lightest neutralino. To get the best signal-to-noise ratio, two different cuts on the non photonic visible energy are choosen:

- $(E_{vis} - E_\gamma) < 0.02 \cdot \sqrt{s}$ for $0.3(0.5) < \Delta(M) < 1$ GeV/c^2
- $(E_{vis} - E_\gamma) < 0.05 \cdot \sqrt{s}$ for $1 < \Delta(M) < 3$ GeV/c^2

The method used to derive the lower limit on the mass of the degenerate chargino is the same applied in [1]; it relies on the bayesian approach and it is described in detail in [15]. In table 3 are listed the 95% CL lower limits on the mass of the degenerate chargino: in correspondence of any of the three scenarios considered, two different limits are reported, one for $0.3 < \Delta(M) < 1$ GeV/c^2 and the other for $1 < \Delta(M) < 3$ GeV/c^2.

	$\lvert\mu\rvert \ll M_2$	$\lvert\mu\rvert \gg M_2$ $M(\tilde{\nu}) > 500$ GeV/c^2	$\lvert\mu\rvert \gg M_2$ Any $M(\tilde{\nu}) > M(\tilde{\chi}_1^\pm)$
$0.3 < \Delta(M) < 1.0$ GeV/c^2	48.0 GeV/c^2	62.6 GeV/c^2	
$0.5 < \Delta(M) < 1.0$ GeV/c^2			50.1 GeV/c^2
$1.0 < \Delta(M) < 3.0$ GeV/c^2	50.5 GeV/c^2	64.0 GeV/c^2	49.5 GeV/c^2

Table 3: 95% *CL lower limits on the mass of the chargino in the three scenarios in which a mass degeneracy with the neutralino is possible.*

Figure 7 compares these limits with the ones obtained in the search for high $\Delta(M)$ charginos in DELPHI [2] and with those obtained with the search for long-lived charginos, as reported in the second reference of [1] and updated preliminarly with the new lifetime calculation and the inclusion of the 1997 statistics in the search for heavy stable charged particles [16]. In the third plot of the figure, the constraint $M(\tilde{\nu}) > M(\tilde{\chi}_1^\pm) + 2$ GeV/c^2 applies on the limits from the long lived particles only: in fact, the limit obtained from this search of radiative, degenerate charginos is valid for any $M(\tilde{\nu}) > M(\tilde{\chi}_1^\pm)$.

All these results take into account a variation of $\tan\beta$ between 1 and 50; the mass of the sneutrino above $M(\tilde{\chi}_1^+)$ (above 500 GeV/c^2 for the gaugino-like scenario at high $M(\tilde{\nu})$); the M_2 and μ parameters chosen so that the mass difference between the chargino and the neutralino remains inside the 0.3-3 GeV/c^2 interval and $M_2 \leq 2M_1 \leq 10M_2$.

6 Conclusions

An update of the search for charginos mass-degenerate with the lightest neutralino has been made using all the data collected by the DELPHI experiment during the runs of

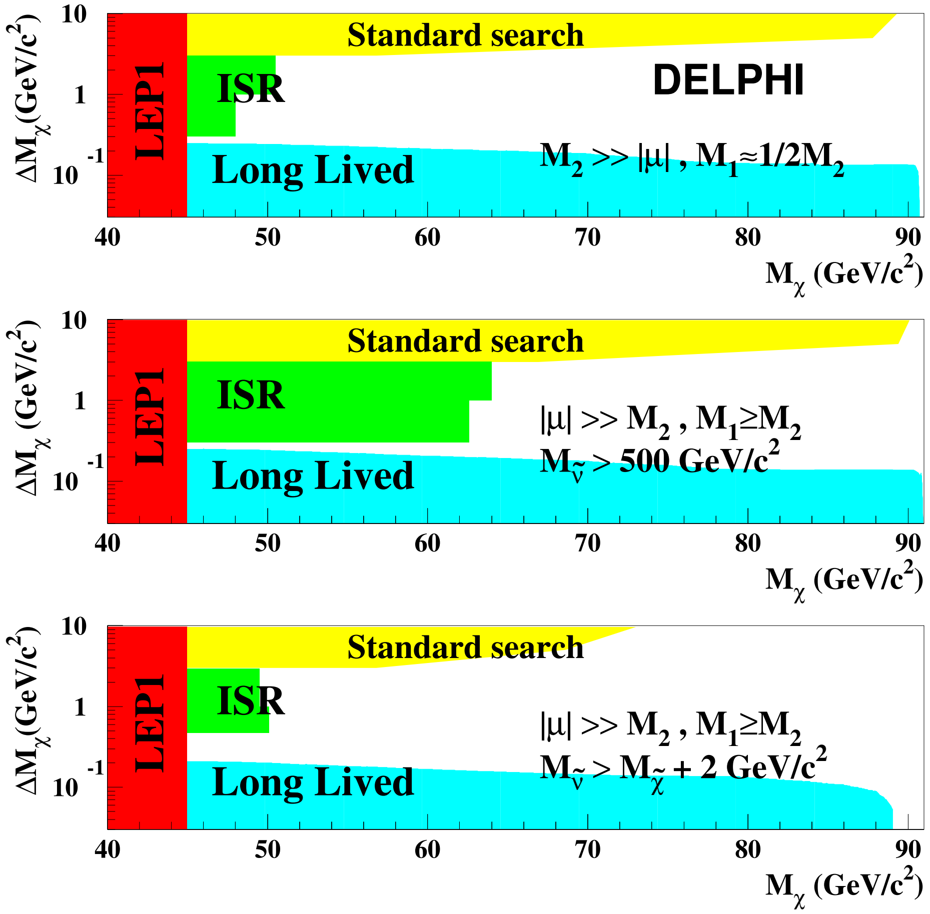

Figure 7: *Regions in the plane* $(M(\tilde{\chi}_1^\pm),\Delta(M))$ *excluded at the 95% CL by the search for high* $\Delta(M)$ *charginos, the present search, and the search for long-lived charginos in the three scenarios where: the lightest chargino is an higgsino; the lightest chargino is a gaugino and* $M(\tilde{\nu}) > 500$ *GeV/*c^2*; the lightest chargino is a gaugino and* $M(\tilde{\nu}) > M(\tilde{\chi}_1^\pm)$.

LEP above the Z^0 pole energy until 1997. When using the initial state photon radiation tag, the otherwise overwhelming two photon background can be reduced to acceptable rates, although such a tag also strongly affects the efficiency of the signal searched for.

To reach a significant sensitivity, all the statistics collected so far at the different LEP2 centre-of-mass energies must be combined together. Such a combination is certainly model dependent (the cross-section behaviour at the different centre-of-mass energies must be taken into account). However, since no evidence of signal has been found, limits has been derived on the mass of the lightest chargino in all the scenarios allowing mass degeneracy with the lightest neutralino.

Acknowledgements

We are grateful to M. Verlato for the help in implementing his routine in our analysis of 1997 data and to P. Ferrari and V. Hedberg for providing us their code for the charge

tag in the STIC Veto. We thank also M. Drees for sending us the correction to the code dealing with the chargino decays at low $\Delta(M)$.

References

[1] S. Paiano, A. Perrotta, T. Rovelli, M. Verardi, DELPHI 97-33 PHYS 686;
C. Lacasta, F.L. Navarria, S.Navas, S. Paiano, A. Perrotta, P. Rebecchi, T. Rovelli, M. Verardi, DELPHI 97-90 CONF 76 , HEP97-427

[2] P. Abreu, et al. (DELPHI coll.) E. Phys. J. **C1** (1998) 1.

[3] C.H. Chen, M. Drees, J.F. Gunion, Phys. Rev. Lett. **76** (1996) 2002;
C.H. Chen, M. Drees, J.F. Gunion, Phys. Rev. **D76** (1997) 330.

[4] M. Drees, private communication.

[5] T. Sjöstrand, Comp. Phys. Comm. **39** (1986) 347;
T. Sjöstrand, CERN-TH/6488/92.

[6] DELPHI 89-15 PROG 130 and DELPHI 89-69 PROG 143.

[7] S. Katsanevas and S. Melanchroinos in "Physics at LEP2", CERN 96-01 (Vol.2) 328.

[8] F.A. Berends, P.H. Daverveldt, R. Kleiss, Nucl. Phys. **B253** (1985) 421;
Comp. Phys. Comm. **40** (1986) 271, 285 and 309.

[9] S. Nova, A. Olshevskyi, T. Todorov, DELPHI 90-35 PROG 152.

[10] M. Verlato, http://wwwcn.cern.ch/ verlato/vft/siveto.html.

[11] M. Feindt, C. Kreuter, O. Podobrin, DELPHI 96-82 PROG 217.

[12] P. Ferrari, V. Hedberg, DELPHI note in preparation.

[13] V. Bocci, et al., Nucl. Inst. Meth. **A362** (1995) 361;
V. Canale, G. Valenti, DELPHI 96-104 DAS 179.

[14] S. Paiano, A. Perrotta, DELPHI 98-37 CAL 139.

[15] V.F.Obraztsov, Nucl. Inst. Meth. **A316** (1992) 388;
A. Perrotta, DELPHI 97-36 PHYS 689.

[16] P. Kluit, U. Schwickerath, DELPHI contribution to Moriond '98.